

1 **A users guide to Neoproterozoic geochronology**

2

3 Daniel J. Condon¹ and Samuel A. Bowring²

4 1. NERC Isotope Geoscience Laboratories, British Geological Survey, Keyworth,
5 NG12 5GS, UK

6 2. Department of Earth, Atmospheric and Planetary Sciences, Massachusetts Institute
7 of Technology, Cambridge, Ma 02139, USA

8 Email – dcondon@bgs.ac.uk

9

10 **Chapter summary**

11 Radio-isotopic dating techniques provide temporal constraints for Neoproterozoic
12 stratigraphy. Here we review the different types of materials (rocks and minerals) that
13 can be (and have been) used to yield geochronological constraints on
14 [Neoproterozoic] sedimentary successions, as well as review the different analytical
15 methodologies employed. The uncertainties associated with a date are often ignored
16 but are crucial when attempting to synthesise all existing data that are of variable
17 quality. In this contribution we outline the major sources of uncertainty, their
18 magnitude and the assumptions that often underpin them.

19 **1. Introduction**

20 Key to understanding the nature and causes of Neoproterozoic climate fluctuations
21 and links with biological evolution is our ability to precisely correlate and sequence
22 disparate stratigraphic sections. Relative ages of events can be established within
23 single sections or by regional correlation using litho-, chemo- and/or biostratigraphy.
24 However, relative chronologies do not allow testing of the synchronicity of events, the
25 validity of correlations or determining rates of change/duration of events. At present,
26 the major limitation to our understanding of the Neoproterozoic Earth System is the
27 dearth of high-precision, high-accuracy, radio-isotopic dates. However, the increase
28 in geochronological constraints over the past five years demonstrates that progress is
29 being made.

30 This chapter outlines the radio-isotopic dating techniques used for the dating of
31 [Neoproterozoic] sedimentary rocks. It is aimed at the many geologists, climate
32 modellers, palaeobiologists and geophysicists, who use Neoproterozoic
33 geochronology, especially those less familiar with the process of obtaining a date
34 from a rock. We provide an outline of the strengths, weaknesses and limitations of
35 the different techniques as well as critical evaluation of the assumptions that underpin
36 the accuracy and precision of the calculated dates and uncertainties. There is an
37 emphasis on U-Pb (zircon) geochronology that reflects its prevalence in the current
38 published literature. We have also tried to place an emphasis on the 'isochron
39 geochronometers' (Re-Os, Lu-Hf and Pb-Pb) applied directly to sedimentary rocks as
40 they are proving to be critical in the direct dating of sedimentary using that are devoid
41 of extrusive igneous rocks. Although the K-Ar and $^{40}\text{Ar}/^{39}\text{Ar}$ are mainstays of
42 Phanerozoic timescale calibration, there are few examples where they have been
43 applied to Neoproterozoic strata. This is most likely due to the susceptibility of K
44 bearing minerals to alteration and argon loss.

45

46 **2. Dateable rocks and minerals**

47 Traditionally the absolute age of sedimentary successions are determined via radio-
48 isotopic dating of uranium and potassium bearing minerals (zircon and sanidine) from
49 volcanic rocks via U-Pb and K-Ar/ ^{40}Ar - ^{39}Ar techniques. These minerals crystallise at
50 (or close to) the time of the magmatic eruption and therefore the age of the mineral is

51 assumed to approximate the depositional age of the volcanic rock. It is also possible
52 to apply radio-isotopic dating to certain sedimentary deposits (chemical precipitates
53 and organic residues) providing they have an elevated parent/daughter ratio and that
54 any initial daughter nuclide can be accounted for (see section 3.2).

55 ***2.1 Dating accessory minerals from volcanic rocks***

56 Zircon (ZrSiO_4) is a common accessory mineral in volcanic rocks ranging from lavas
57 to air-fall tuffs and is a nearly ubiquitous component of most clastic sedimentary
58 rocks. The most common volcanic rocks in fossil-bearing sequences are air-fall
59 layers deposited in marine settings that range in thickness from a millimeter to many
60 meters. In most of these rocks the primary volcanic material has been altered,
61 probably soon after deposition, to clay minerals in a process that has little effect on
62 zircon. The refractory and durable nature of zircon over a wide range of geological
63 conditions means that it is likely for zircon to remain a robust indicator of magmatic
64 events even through subsequent metamorphism. What makes zircon ideal for U-Pb
65 dating is that because U has a similar charge and ionic radius to Zr it substitutes
66 readily into the zircon crystal structure (in modest amounts, typically in the 10's to
67 hundreds of ppm range) whereas Pb has a different charge and larger ionic radius
68 leading to its effective disclusion from the crystal lattice. Therefore at t_0 there is
69 effectively no Pb present in the crystal (although mineral and fluid inclusions may
70 contain both common and radiogenic Pb). An additional factor that makes zircon
71 such a robust chronometer is its high closure temperature ($>900^\circ\text{C}$), the temperature
72 below the zircons are effectively sealed and U and Pb do not undergo thermally
73 activated volume diffusion. This means that zircons preserve their primary ages even
74 in volcanic rocks contained in amphibolite facies metasedimentary successions (e.g.,
75 Hoffmann et al., 2004).

76 The refractory and durable nature of zircon means that it is often recycled through
77 crustal processes of erosions, metamorphism and magmatism, which combined with
78 its high closure temperature means that it is possible to inherit older zircon in newly
79 formed igneous rocks. This commonly occurs as older cores surrounded by a rim of
80 younger, magmatic zircon. Such grains pose an analytical challenge in that the
81 different domains need to be analysed separately, which is best achieved using either
82 microbeam techniques (see section 4.2) that employ ion beams and lasers to micro-

83 sample different domains within a single zircon crystal or micro sampling of single
84 grains followed by conventional analysis.

85 A further complication arises when one considers that the crystallization history of a
86 magma is not always an instantaneous event and that in certain circumstances (such as
87 large volume silicic eruptions) zircons may crystallize several tens of thousands of
88 years prior to eruption and/or over a protracted interval. Furthermore, in long-lived
89 magmatic systems it is possible that older material is cannibalized and that zircons in
90 an air fall tuff may record a continuum of dates from eruption up to several million
91 years before. In such situations high-precision single grain analyses are required in
92 order to deconvolve the complexity within a population and to assign an age to the
93 sample.

94 It is also possible to date other accessory phases from volcanic ash beds such as
95 monazite and titanites, however these are much less common in their occurrence than
96 zircon. Monazite [(LREE)PO₄] is typical of peraluminous magmas and metamorphic
97 rocks, however it also rarely found in volcanic ash beds (reference). Monazite has a
98 similarly high closure temperature (>900°C) to zircon and in addition to incorporating
99 uranium into its crystal lattice will incorporate ThO₂ at the percent level making it
100 ideally suited to Th-Pb dating. Titanite (sphene) (CaTiSiO₅) is a common accessory
101 phases in metamorphic rocks, and somewhat less common in plutonic and volcanic
102 rocks. The advantage of titanite is that it has a moderate closure temperature (ca.
103 650°C) that means it does not accumulate Pb until it cools below that temperature. In
104 the case of volcanic rocks equates to the eruption event and therefore pre-eruptive
105 residence of titanite is not a limiting factor for its use in dating volcanic eruptions.
106 Unfortunately, titanite also incorporates some Pb into its crystal structure resulting in
107 moderate initial common Pb that limits the precision of titanite U/Pb dates.

108 ***2.2 Dating chemical precipitates and organic residues***

109 It is becoming increasingly apparent that chemically precipitated rocks and organic
110 residues from sedimentary rocks can serve as chronometers using the isochron
111 approach and calculated dates are interpreted to approximate the time of
112 sedimentation and/or early diagenesis. The most commonly applied chronometers in
113 Neoproterozoic rocks include carbonates, phosphates and organic-rich shales, as they
114 contain high concentrations of the various parent nuclides (Re, U and Lu etc.).

115 *2.2.1 U-Pb dating of carbonates*

116 At the time of formation, carbonates can incorporate uranium into their crystal lattice,
117 typically with several parts per million (ppm) concentration (although in some cases
118 this can be many tens of ppm), as well as (initial) Pb with concentrations typically in
119 the ppb range, and therefore have the potential for U-Pb dating. Carbonates form in a
120 variety of terrestrial and marine environments however Neoproterozoic successions
121 targeted for U-Pb dating are invariably marine. Fluid mediated recrystallisation of
122 carbonates is a common processes during burial and metamorphism and very few (if
123 any) Neoproterozoic carbonates are pristine. Whilst fluids are unlikely to cause
124 isotopic fractionation the variable solubility of Pb and U means that it is common for
125 the two to become uncoupled, in which case the U-Pb systematics are somewhat
126 unreliable and the Pb-Pb system is relied upon for age information. Several studies
127 have generated Pb-Pb isochrons from Neoproterozoic successions with varying
128 success and most studies finding significant evidence for disturbance of the Pb-Pb
129 systematics during subsequent burial/metamorphic events (Babinski et al., 1999;
130 Babinski et al., 2007). Recent studies have been successfully employing combined
131 textural and Sr isotope analyses of the carbonates as an independent proxy for
132 disturbance during fluid flow events (Babinski et al., 2007).

133 *2.2.2 Re-Os dating of organic-rich sediments*

134 Both Re and Os become concentrated within anoxic sediments by redox reactions
135 close to the sediment-water interface and are known to be incorporated in the organic
136 matter of organic rich shales (Creaser et al., 2002). Furthermore, both Re and Os are
137 apparently hydrogenous in nature and following deposition they can act as a closed
138 system allowing for their exploitation for geochronology. In the past 5 years the Re-
139 Os geochronometer has been applied to several organic rich
140 Neoproterozoic stratigraphic intervals (Kendall et al., 2006; Kendall et al., 2004;
141 Schaefer and Burgess, 2003). Studies of the greenschist facies Old Fort Point
142 Formation (Kendall et al., 2004) suggests that Re-Os systematics can remain coherent
143 during low grade metamorphism.

144 *2.2.3 U-Pb and Lu-Hf dating of phosphates*

145 Phosphates are known for their enrichment (relative to the fluid from which they
146 precipitate) in rare earth elements (REE), thorium and uranium thus allowing for

147 potential use as geochronometer through exploitation of the Lu-Hf, Th-Pb and U-Pb
148 decay schemes. Few studies have yet to exploit the Lu-Hf and U-Pb system for the
149 dating of sedimentary phosphates. Barfod et al (Barfod et al., 2002) presented a
150 combined U-Pb and Lu-Hf isochron study of the Douhantuo phosphorites obtaining a
151 Lu-Hf 'isochrons' at ca. 600 Ma (uncertainties of 26 to 81 Ma and MSWDs from 2.0
152 to 25) and a Pb-Pb isochron of 599.3 ± 4.2 Ma ($n = 5$, MSWD = 2.9). These dates are
153 consistent with U-Pb zircon dates from the top and bottom of the Doushantuo
154 formation (Condon et al., 2005), however all 'isochrons' recorded excess scatter.
155 This scatter was attributed to the presence of detrital clays that were not fully
156 eliminated despite sample pre-treatment to remove clay fractions.

157 In addition to dating 'bulk' phosphates, both monazite and xenotime (YPO_4) are
158 known to form during early diagenesis (Evans et al., 2002; Rasmussen, 2005). Both
159 minerals have highly favourable U/Pb systematics and are robust phases however
160 their form within the sediments makes them difficult to analyse. Xenotime occurs as
161 syntaxial overgrowths on zircons but due to their small size (a few 10's of μm), and
162 textural complexity, an *in-situ* isotopic technique with a spatial resolution of $<10 \mu\text{m}$
163 is required to successfully date xenotime; to date, this has only been achieved by ion
164 microprobe. In addition, precipitation of xenotime also occurs during fluid and
165 thermal events adding a further layer of complication if the timing of sedimentation is
166 the target. In contrast to xenotime, diagenetic monazite tends to occur as nodules (up
167 to 2mm diameter) in shales. Studies of Palaeozoic diagenetic monazites nodules have
168 demonstrated that the Pb-Pb and Th-Pb systems are robust however the U-Pb has
169 been perturbed indicating U remobilization (Evans et al., 2002). Neither (diagenetic)
170 monazite or xenotime U-Pb geochronology have (yet) been successfully have been
171 successfully applied to the dating of a Neoproterozoic sedimentary succession.

172 The 'isochron geochronometers' are invaluable for obtaining age information from
173 sedimentary successions devoid of volcanic material that can be dated by the U-Pb
174 zircon method. Despite the large uncertainties intrinsic to the dating of these types of
175 materials, techniques such as the Pb-Pb isochron method are providing critical in
176 providing age information for stratigraphic intervals that are devoid of volcanic units
177 for U-Pb (zircon) dating (Babinski et al., 2007; Barfod et al., 2002). Uncertainties on
178 Re-Os isochron dates are now yielding uncertainties comparable to U-Pb (zircon)
179 microbeam dates. Issues relating to the isochron geochronometers are centred around

180 the lack an independent check on open-system behaviour. Quite often the MSWD
181 and agreement with existing constraints are used to assess accuracy, if ages are
182 younger than a minimum age constraint then the isochron date must reflect a fluid
183 event. For the Pb-Pb method applied to carbonates, the evaluation of the Sr isotopes
184 may serve as a good proxy for disturbance (or lack thereof).

185

186 *2.3 Maximum and minimum age constraints*

187 Not all sedimentary successions are amenable to direct dating via radio-isotopic
188 methods. In the absence of zircon bearing volcanic rocks, or chemical sediments for
189 isochron dating, another approach is to obtain maximum age constraints by the dating
190 of detrital zircons. Detrital zircons in clastic rocks can range from being considerably
191 older than the estimated age of the sedimentary rock they are contained within (often
192 many hundreds of millions of years older) to close to the age of sedimentation and in
193 this case can provide valuable constraints (Bingen et al., 2005). Minimum age
194 constraints can be provided by overlying strata (which may contain age-diagnostic
195 fossils) and/or cross-cutting igneous intrusions. If a radio-isotopic date provides the
196 age control then the issues outlined in this chapter will apply. When the radio-
197 isotopic constraint is somewhat temporally distant from the presumed age of the
198 sediment there is a tendency to ignore the age uncertainties but this can sometimes be
199 misleading (see section 5 for further discussion).

200

201 **3. Radio-isotopic geochronometers**

202 A relatively small number of radioactive decay systems are suitable for dating
203 Neoproterozoic rocks due to their long half-lives and are listed in table 1. All of these
204 systems are based upon the radioactive decay of a parent nuclide to a stable daughter
205 nuclide. Exploiting these decay systems for the purposes of determining the age of a
206 mineral or rock is dependent upon (1) the decay constant of the parent nuclide must
207 be accurately and precisely determined; (2) closed system behaviour, which can be
208 simply stated to mean there has been no loss or gain of parent or daughter nuclide
209 since formation (or ‘closure’) of the material, and (3) the initial daughter nuclide, if
210 present, can be precisely and accurately accounted for. In this section we outline the
211 basic principles of the various radio-isotopic geochronometers, differentiating the U-

212 Pb system applied to U-bearing accessory minerals from the isochron
 213 geochronometers (Re-Os, Lu-Hf, Pb-Pb etc.) applied to chemical precipitates and
 214 organic residues.

Radioactive Parent Nuclide	Radiogenic Daughter Nuclide	Half life (yrs)
^{238}U	^{206}Pb	4.468×10^9
^{235}U	^{207}Pb	7.038×10^8
^{187}Re	^{187}Os	4.16×10^{10}
^{176}Lu	^{176}Hf	3.71×10^{10}
^{87}Rb	^{86}Sr	4.944×10^{10}
^{40}K	$^{40}\text{Ar}, ^{40}\text{Ca}$	1.25×10^9

215 **Table 1.** Radiometric decay systems used in geochronology.

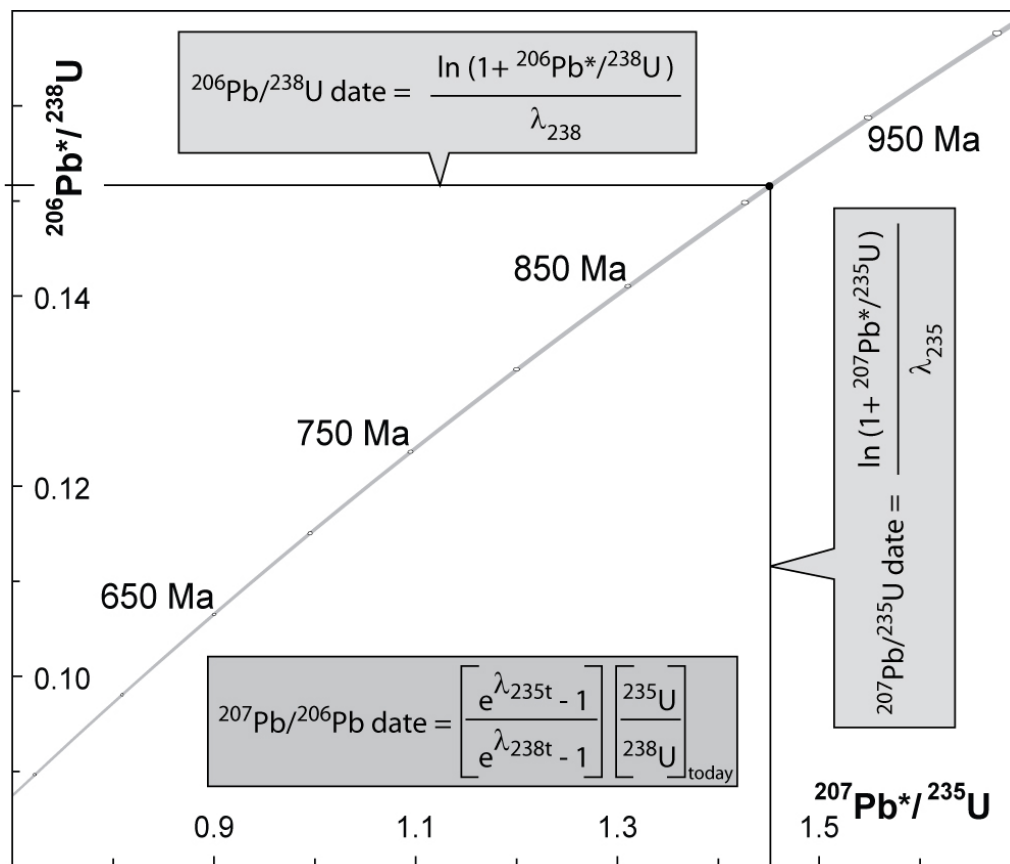
216

217 **3.1 Uranium-Lead**

218 U-Pb geochronology is often regarded as the gold standard of geochronology because
 219 unlike all other chronometers it exploits two independent decay schemes, ^{235}U to
 220 ^{207}Pb and ^{238}U to ^{206}Pb and ^{238}U and ^{235}U decay constants are relatively precise (Jaffey
 221 et al., 1971). Two separate dates for a zircon based on each individual decay schemes
 222 may be calculated and visualised using the concordia diagram (Fig. 1). On a
 223 conventional (Wetherill) concordia diagram the X and Y axis are the $^{207}\text{Pb}/^{235}\text{U}$ and
 224 $^{206}\text{Pb}/^{238}\text{U}$ ratios respectively, and the concordia curve represents the simultaneous
 225 solution of the decay equations for a given age. A third ^{207}Pb - ^{206}Pb date can be
 226 determined from only Pb isotopic measurements through knowing both the ^{235}U and
 227 ^{238}U decay constants and the present day $^{235}\text{U}/^{238}\text{U}$ ratio which is assumed invariant at
 228 ca. 137.88. Calculation of the U/Pb dates requires determination of the Pb*/U ratio
 229 (Pb* denotes radiogenic Pb) and the corresponding decay U constant. See Fig. 1 for
 230 age equations.

231 The advantage of two independent chronometers in the same mineral is that it is
 232 possible to detect small amounts of open system behaviour such as Pb loss or the
 233 inheritance of older material. This is a major factor in our ability to make reliable,
 234 high-precision age determinations as we can evaluate whether a number of analyses
 235 represents a time of mineral growth. The different half lives of ^{238}U and ^{235}U , ca. 4.5

236 and ca. 0.7 Ga respectively, combined with their varying abundances in nature, means
 237 that much smaller amounts of ^{207}Pb are produced per increment of time in the
 238 Neoproterozoic. Although all three dates can be calculated from most published
 239 analyses, the relative precisions are related to the analytical technique employed (see
 240 section 5 for further discussion of age uncertainties). The U-Pb method is most-often
 241 applied to U-bearing accessory minerals such as zircon found in igneous rocks but it
 242 has also been applied to both carbonates and phosphorites using Pb-Pb isochrones
 243 where the initial Pb contribution is significant.

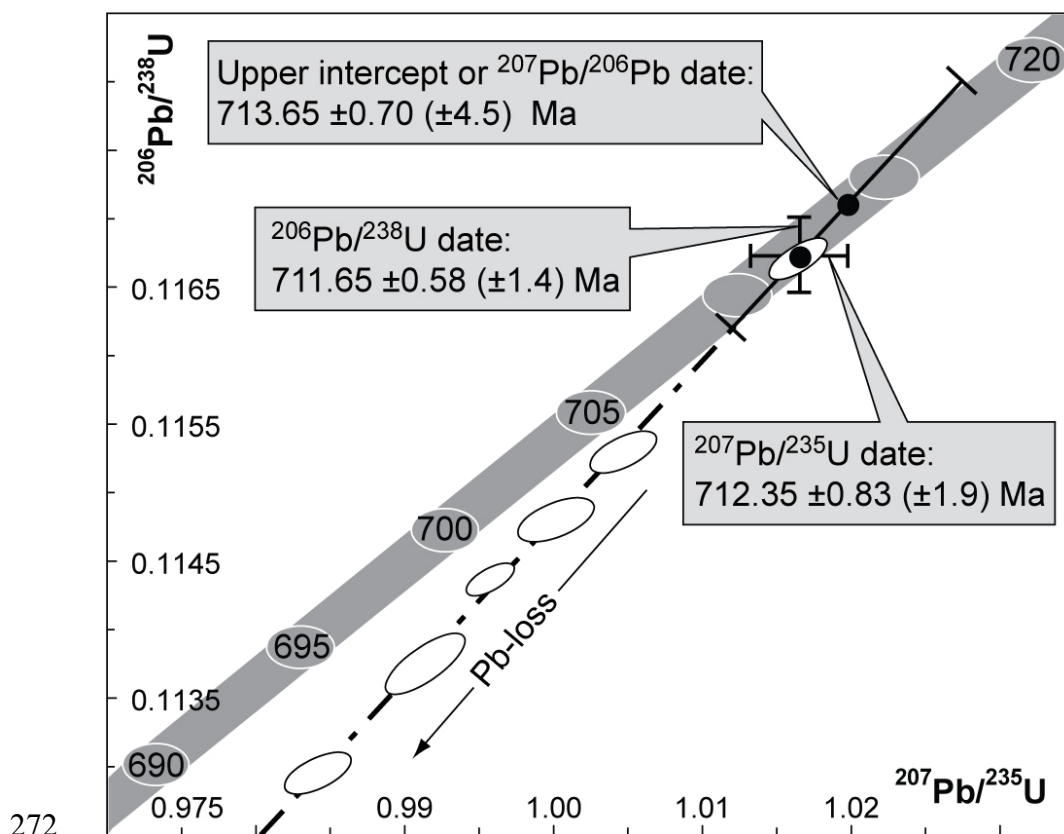


245 **Figure 1.** U-Pb (Wetherill) concordia diagram for the age range 542 to 1000 Ma. The grey band
 246 represents the concordia curve plotted to reflect the uncertainties in the ^{235}U and ^{238}U decay constants.
 247 Unfilled ellipses are plotted at 50 Myr intervals. λ = decay constant.

248

249 Assuming that zircon crystallization and deposition of an ash are approximately
 250 simultaneous, is it correct to assume that the calculated radio-isotopic dates be
 251 assumed to accurately date the time of zircon crystallisation or stated another way, has
 252 the zircon remained a closed system? It has been known for several decades that
 253 zircons often show evidence for post-crystallisation Pb-loss. This has the effect of

254 lowering the U/Pb ratios and the derived dates (see Fig. 2). In order to
 255 minimise/eliminate the effects of post-crystallisation Pb-loss it is possible to subject
 256 zircons to pre-treatment techniques in order to physically remove the domains that
 257 have suffered Pb-loss thus increasing the probability of closed system behaviour. The
 258 first approach was to physically abrade away the exterior portions of the zircons
 259 (Krogh, 1982a), based on the observation that the outer portions were richest in U and
 260 thus susceptible to radiation damage and Pb-loss. At the same time Krogh (Krogh,
 261 1982b) also suggested the selection of the most non-magnetic zircons as they
 262 corresponded to lowest U contents and had least amount of Pb-loss. These
 263 approaches were widely applied until the development of a new technique described
 264 as ‘chemical abrasion’ (Mattinson, 2005). This technique involves annealing zircon
 265 grains at 800-900 °C followed by partial dissolution. This method effectively “mines
 266 out” the higher U parts of the zircon that have been damaged by radiation and are thus
 267 susceptible to fast-pathway diffusion of Pb from the zircon crystal. This method
 268 seems to offer the promise of total elimination of open system behaviour in most
 269 zircon. Microbeam techniques (see section 4.1.2) have not typically employed pre-
 270 treatment techniques as they assume that Pb-loss is restricted to the exterior portions
 271 of grains which they attempt to avoid during the in-situ analyses.



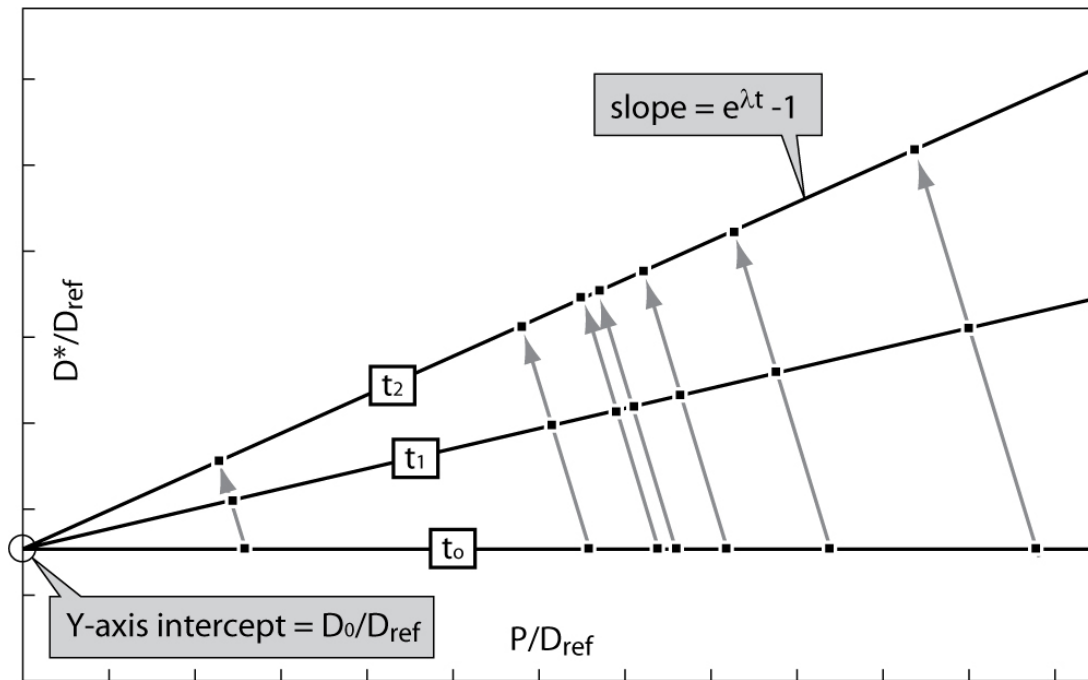
273 **Figure. 2.** Schematic U-Pb concordia diagram illustrating the $^{206}\text{Pb}/^{238}\text{U}$, $^{207}\text{Pb}/^{235}\text{U}$ and $^{207}\text{Pb}/^{206}\text{Pb}$
274 dates can be calculated. The data presented is a subset of analyses from sample WM54 (Bowring et al.,
275 2007). Uncertainties are the 2σ internal uncertainties those in parenthesis are the 2σ internal plus the
276 systematic decay constant uncertainties; 0.11% for ^{238}U and 0.14% for ^{235}U (Jaffey et al., 1971). The
277 grey band is the concordia line plotted to reflect the uncertainties in the U decay constants. Error
278 ellipses (white) are plotted with 2σ internal uncertainties, black error bars represent 2σ internal plus the
279 systematic decay constant uncertainties.

280

281 **3.2 'Isochron goeochronometers' (Re-Os, Lu-Hf, Pb-Pb etc.).**

282 The isochron method involves the analyses of multiple cogenetic samples (minerals or
283 sub-samples of a rock from a stratigraphic interval) and is used when an initial
284 amount of daughter atoms may be present and there is the possibility of a range in
285 Parent/daughter. This is the situation for the Re-Os, Lu-Hf and U-Pb chronometers
286 applied to carbonates, phosphates and organic-rich shales which tend to incorporate
287 an both parent and daughter isotopes at the time of their formation. Ideally, the
288 isochron approach allows determination of both an age and an initial isotopic
289 composition of the daughter element that can be used to identify its source (i.e.,
290 mantle vs crust) and track changes in seawater chemistry.

291 For multiple, cogenetic samples to preserve the time of system closure, samples must
292 begin with (1) a homogenous initial daughter isotopic composition, and (2) a spread in
293 parent/daughter ratio such that over time different samples with a range in
294 parent/daughter will fall on a straight line whose slope is equal to $e^{\lambda t} - 1$ (Fig. 3). A
295 typical isochron is plotted P/D_{ref} on the X axis and D^*/D_{ref} on the Y axis, where P is
296 the number of parent atoms in sample, D_{ref} is the number of atoms of a stable
297 reference isotope of the daughter element and D^* is the total number of radiogenic
298 daughter atoms plus initial atoms of the same isotope (amount of daughter atoms due
299 to decay = $D^* - D_0$) (Fig. 3). At the time of sample formation (t_0) all samples should
300 plot on a horizontal line, however as the parent decays over time (t_1, t_2 , etc.) each
301 sample will evolve along a slope of -1 and samples with higher initial parent/daughter
302 ratio (P/D_{ref}) will be displaced the most (Fig. 3) such that the isochron rotates to a
303 positive slope. Assuming closed system behaviour since the formation of the sample,
304 a linear regression through the points allows calculation of the slope and y-intercept
305 from which the age and the initial isotopic composition of the daughter can be
306 determined (Fig. 3).



307

308 **Figure 3.** Schematic isochron diagram illustrating (1) the situation at t_0 where different samples from
 309 the same stratigraphic interval record a spread in parent(P)/daughter(D_{ref}) ratios but a constant initial
 310 daughter isotopic composition. D_0 is the initial amount of the daughter isotope and D^* is the
 311 radiogenic daughter isotope (from decay and initial) such that the daughter produced solely from decay
 312 (since t_0) = $D^* - D_0$.

313

314 **4. Analytical methodologies**

315 The majority of age constraints for Neoproterozoic strata are derived from U-Pb
 316 zircon dates therefore most of this section is concerned with U-Pb analytical
 317 methodologies. The analytical methodologies used for the ‘isochron
 318 geochronometers’ are somewhat similar to ID-TIMS U-Pb method however the
 319 differences are discussed below.

320 **4.1 U-Pb methodologies**

321 There are two main approaches to U-Pb zircon geochronology: in-situ ‘microbeam’
 322 techniques and isotope dilution thermal ionization mass spectrometry (ID-TIMS). The
 323 major difference is that in ID-TIMS geochronology, zircon is dissolved and the U and
 324 Pb separated from the other elements prior to analysis whereas in microbeam
 325 techniques the zircon is analyzed by a laser or ion beam in a sectioned and polished
 326 epoxy mount or thin section.

327 **4.1.2 U-Pb ID-TIMS**

328 ID-TIMS analyses of zircon (either as multi-grain fractions, single grains or grain
329 fragments) involves dissolution of the zircon in the presence of tracer isotopes called
330 isotope dilution. For U-Pb ID-TIMS analyses the most common tracers are ^{205}Pb and
331 ^{235}U . ^{205}Pb is an artificial tracer that does not occur in nature whereas ^{235}U is natural
332 however its abundance to ^{238}U is assumed to be constant with $^{235}\text{U}/^{238}\text{U} = 137.88$
333 therefore it can be used to determine the number of moles of ^{238}U and ^{235}U .
334 Following dissolution the sample undergoes chemical purification using anion
335 exchange chemistry that allows separation of the Zr and REEs from the Pb and U, and
336 Pb and U from one another.

337 Following purification Pb and U are analysed separately by thermal ionisation mass
338 spectrometry where the sample isotopes (^{204}Pb , ^{206}Pb , ^{238}U , etc) can be ratio-ed
339 against the tracer isotope (^{205}Pb , ^{235}U) and the number of atoms of each naturally
340 occurring isotope in the sample can be determined. Because the ratio of tracer
341 isotopes to isotopes in the rock or mineral are established before any processing,
342 inefficient separation of U and Pb and typically low ionisation efficiency of U and Pb
343 do not affect the ratios and ultimately the age. After corrections for mass
344 fractionation, the minor contribution of common Pb and U from the reagents, the
345 tracer and labware, the sample $^{206}\text{Pb}/^{207}\text{Pb}$, $^{206}\text{Pb}/^{238}\text{U}$ and $^{207}\text{Pb}/^{235}\text{U}$ ratios can be
346 determined and $^{206}\text{Pb}/^{207}\text{Pb}$, $^{206}\text{Pb}/^{238}\text{U}$ and $^{207}\text{Pb}/^{235}\text{U}$ dates calculated.

347 Optimisation of this technique means that it is now possible to date zircons with <10
348 pg radiogenic Pb and obtain precision <0.1% on the U/Pb ratio for single grain
349 analyses. However, it is a very time consuming technique, each single U/Pb analyses
350 takes several hours of mass-spectrometry, making it difficult to develop high-*n*
351 datasets.

352

353 *4.1.3 U-Pb Microbeam techniques*

354 U-Pb geochronology by microbeam techniques has revolutionized geochronology
355 over the past two decades. The two major techniques are Secondary Ion Mass
356 Spectrometry (SIMS), typified by the SHRIMP (Sensitive High Resolution Ion
357 Microprobe), and Laser Ablation Inductively Coupled Plasma Mass Spectrometry
358 (LA-ICP-MS). Both of these techniques (collectively termed ‘microbeam’ techniques)
359 offer high-spatial resolution analyses using either a focused ion beam to sputter a

360 volume of zircon (SIMS) or a laser that is used to vaporise a volume of zircon (LA-
361 ICP-MS). Microbeam techniques allow in-situ analysis of very small volumes and
362 thus high-spatial resolution; a typical volume of zircon analyzed by an ion-probe is
363 cylindrical, 20-30 microns in diameter and several microns deep, with somewhat
364 larger volumes for LA-ICPMS (Kosler and Sylvester, 2003). In addition the analyses
365 can be done relatively rapidly (many 10's analyses per day for LA-ICPMS and
366 SIMS). Furthermore, these techniques allow analysis of remaining mineral for other
367 isotopes/elements of interest (Hf, O, REE's) can be made on the same zircon grains in
368 close proximity to the volume analyzed for geochronology.

369 Fundamental to the microbeam U-Pb zircon methods is use of a primary standard
370 against which the U/Pb ratio of the unknown zircon is calibrated. For SIMS
371 techniques this calibration involves the analyses of standard zircon to develop a
372 calibration curve for a known U/Pb ratio (which is determined via ID-TIMS analyses)
373 and against which analyses of unknown zircons can be compared. This is achieved
374 through analytical sessions where a standard zircon is repeatedly analysed
375 interspersed with analyses of unknown zircons (this is termed sample-standard
376 bracketing). For LA-ICPMS the approach is somewhat similar manner in that sample-
377 standard bracketing is employed in order to determine the interelemental fractionation
378 which is then applied to the unknown zircons. In both SIMS and LA-ICPMS
379 techniques the $^{207}\text{Pb}/^{206}\text{Pb}$ ratio is a direct measurement, for SIMS mass-dependent
380 fractionation appears to be minimal and the measured ratio is commonly used whereas
381 in LA-ICPMS analyses mass dependent fractionation is quantifiable and is corrected
382 for either using sample-standard bracketing and/or using a solution with known
383 $^{205}\text{Tl}/^{203}\text{Tl}$ ratio to correct for mass bias on Pb isotopic ratios. For further details of
384 microbeam techniques see Ireland and Williams (Ireland and Williams, 2003) for a
385 review of SIMS U-Pb geochronology and Kosler and Sylvester (Kosler and Sylvester,
386 2003) for a review of LA-ICPMS geochronology.

387 The benefit of the high spatial resolution provided by microbeam techniques is a
388 tradeoff in that the precision of individual spot analyses using LA-ICPMS and SIMS
389 is lower than ID-TIMS by approximately an order of magnitude (Ireland and
390 Williams, 2003; Kosler and Sylvester, 2003). In-situ techniques are without question
391 essential tools for characterizing complex (zoned) zircons from volcanic and

392 metamorphic rocks and for characterizing detrital populations which in some cases
393 can provide robust estimates of the minimum age of a sequence.

394 ***4.2 Isochron techniques***

395 Isochron techniques involve analysis of multiple samples assumed to be the same age,
396 have a spread in parent/daughter ratio, and have remained closed systems. In order to
397 ensure the samples are the same age and have the same initial isotopic composition it
398 is preferable to sample laterally from the same unit (e.g., (Kendall et al., 2004)),
399 minimizing thickness and to avoid integration of samples from a stratigraphic
400 thickness. In some cases, such as working with core samples, this is not always
401 possible (Kendall et al., 2006). This could be a complicating factor if there is
402 temporal variation in the initial isotopic composition of the daughter element, and/or
403 represents a significant amount of time, especially in condensed sections.

404 Sample dissolution and purification are similar to the procedures for U-Pb ID-TIMS.
405 Prior to isotope ratio mass spectrometry samples undergo dissolution and chemical
406 purification. For multi-element systems (such as Re-Os, U-Pb and Lu-Hf) isotopic
407 tracers are added prior to dissolution for the isotope dilution (see above) whereas for
408 single element systems (such as Pb-Pb), direct measurements of the isotope ratios are
409 made. The isotopic composition is determined via thermal ionization mass-
410 spectrometry although it is also possible to use solution mode ICPMS for most
411 elements.

412 The accuracy and precision of isochron techniques is largely controlled by the quality
413 of the rock or mineral itself, primarily a spread in initial parent/daughter ratio, and
414 closed system behaviour. For precipitates such as carbonates and phosphates there is
415 often no significant detrital input however this is not the case for organic rich shales
416 targeted for Re-Os. Because the organic rich shales contain detrital material there is
417 potential that significant concentrations of Os from multiple sources can occur. This
418 has been demonstrated in several studies (Creaser et al., 2002; Kendall et al., 2004)
419 however it is possible to limit the detrital Os contribution by selective dissolution of
420 the organic component using $\text{CrO}_3\text{-H}_2\text{SO}_4$ dissolution approach. Kendall et al
421 (Kendall et al., 2004) compared two dissolution methods (aqua regia vs. $\text{CrO}_3\text{-H}_2\text{SO}_4$
422 dissolution) on greenschist facies organic rich shale from the Old Fort Point
423 Formation in Western Canada. Both dissolution techniques were used on the same

424 powders, however the aqua regia method yielded scattered data and a resulting
425 “isochron” regression with an MSWD of 65 and a large “age” uncertainty (9%) in
426 comparison to the CrO₃-H₂SO₄ dissolution method which yielded an isochron with
427 much less scatter (MSWD = 1.2) and a relatively low uncertainty (0.8% 2σ) (Kendall
428 et al., 2004).

429

430 **5. Sources and types of uncertainty**

431 Without an accurate estimation of uncertainty, the radio-isotopic age of a given rock
432 or mineral is of limited value. For example, suppose a date of 618 Ma is reported for
433 a detrital zircon from a unit that underlies a Marinoan-type glacial deposit? If the date
434 is relatively precise (and accurate), say ± 2 Myr, then it could be inferred that the
435 onset of glacial sediment accumulation post-dates deposition of the detrital material at
436 618 ± 2 Ma. On the other hand, if the 618 Ma date has an uncertainty of 100 Myr then
437 the detrital mineral could be as old as 718 Ma or young as 518 Ma, making it of
438 limited use. Consider the case where the 618 Ma is the ²⁰⁶Pb/²³⁸U date with an
439 uncertainty of 10 Myr but the ²⁰⁷Pb/²⁰⁶Pb date is 650 ± 400 Ma. Although the two
440 dates overlap the concordia curve (and are therefore technically concordant), the lack
441 of precision on the ²⁰⁷Pb/²⁰⁶Pb date renders it impossible to assess open-system
442 behaviour (such as Pb-loss or inheritance) within the limits imposed by the precision
443 of the ²⁰⁷Pb/²⁰⁶Pb date and thus the accuracy of the ²⁰⁶Pb/²³⁸U date is unknown. This
444 later example might at first seem extreme but data of this type exist in the published
445 literature and are often cited. For example, Ireland et al (Ireland et al., 1998)
446 published an extensive dataset of SHRIMP U-Pb zircon dates on detrital zircons from
447 the Kanmantoo Group in Australia (it should be noted that it was not the intention of
448 this study to constrain the timing of sediment accumulation). The units sampled
449 included the Marino Arkose where fifty detrital zircons were analysed, the majority of
450 which were >1 Ga (n =48). Two grains yielded ²⁰⁶Pb/²³⁸U dates of 649 ± 17 and 655
451 ± 17 which many researchers use to indicate that the Marino Arkose is ca. 650 Ma (or
452 younger) (Halverson et al., 2005; Peterson et al., 2005; Zhou et al., 2004). The
453 ²⁰⁷Pb/²⁰⁶Pb dates associated with these two analyses are 470 ± 440 Ma and 666 ± 307
454 Ma respectively. Statistically it is possible that the two zircons are ca. 650 Ma, but
455 the probability is quite low and it is not legitimate to assume the ²⁰⁶Pb/²³⁸U date is an
456 accurate estimate of the age of the zircons without considering both the ²⁰⁶Pb/²³⁸U and

457 $^{206}\text{Pb}/^{207}\text{Pb}$ uncertainties. In practical terms these two detrital zircon dates provide no
458 significant constraint.

459 It is necessary for anyone who uses geochronological data to understand the various
460 sources of error and when one must consider the total uncertainty of a given date as
461 opposed to its constituent parts. Although the uncertainty of each date contains an
462 internal/random component in the total uncertainty, there are also components that are
463 systematic (such as those related to the decay constants). In some circumstances these
464 can be ignored offering a potential increase in resolving power. In this section we
465 review the different sources of uncertainties and the assumptions that underlie the
466 often quoted (or not) errors. For more detailed treatment of uncertainties in
467 geochronology the following articles are recommended: Ireland and Williams (Ireland
468 and Williams, 2003); Stern and Amelin (Stern and Amelin, 2003), Schmitz and
469 Schoene (Schmitz and Schoene, 2007), and various papers by Ludwig (Ludwig, 1980,
470 1991, 1998, 2003).

471 ***5.1 Random/internal uncertainties***

472 Random/internal uncertainties can be considered as those relating to the measurement
473 of isotopic ratios of the sample, standards and blank and are used in the derivation of
474 the radiogenic ratios. Most of these sources of random uncertainty relate to the mass-
475 spectrometry and our ability to measure isotopic ratios with precision and accuracy.
476 Factors such as the electronic noise of detectors place a theoretical limit on the
477 precision which can be achieved by detecting a certain number of ions over a finite
478 period of time. However for almost all geochronologic applications other factors such
479 as correction for mass dependent fractionation that occurs during sample ionisation,
480 and correction for common and/or initial parent and daughter nuclide dominate the
481 analytical uncertainty budget. It is possible to reduce the uncertainty in the mass
482 dependent fractionation via 'double-spiking', where two tracer isotopes of the same
483 element (^{202}Pb - ^{205}Pb , or ^{233}U - ^{235}U for example) are used for real time mass
484 fractionation correction.

485 The analytical uncertainties associated with U-Pb ID-TIMS dates have decreased
486 substantially over the past decade. This is due in large part to a reduction in the
487 common Pb levels introduced in the laboratory, as the isotopic composition of this
488 common Pb is imprecisely determined (due to its variability), therefore the reduction

489 in common Pb levels reduces the uncertainty associated with the common Pb
490 correction. The nature of SIMS and LA-ICPMS (in ‘dry’ mode) analyses means that
491 common Pb levels are intrinsically low.

492 *5.1.1 Microbeam U/Pb standardisation*

493 Microbeam U-Pb dating of zircons is a relative analytical technique where dates are
494 calculated relative to a standard zircon of known age. Microbeam U-Pb data are
495 acquired in analytical sessions where the unknown zircons are analysed in
496 conjunction with the standard zircon of known age. The raw measured U/Pb ratio of
497 the standard varies or “drifts” during an analytical session due to slight changes in
498 instrument parameters. Therefore there is an uncertainty associated with the Pb/U
499 standardisation that has to be considered. This uncertainty is on the order to 1%
500 (Stern and Amelin, 2003), however the accuracy of its quantification is dependent
501 upon the number and frequency with which the standard is analysed.

502 There are differences of opinion on how the uncertainty related to the U/Pb
503 standardisation is factored into the total uncertainty of a date. Some groups consider
504 that the ‘standardisation’ value is constant for a given session and therefore the
505 uncertainty is systematic and needs only be considered when comparing data
506 collected in different analytical sessions (if this is correct then the session Pb/U
507 uncertainty can be simply added to the weighted mean uncertainty in a manner
508 analogous to the ID-TIMS tracer calibration uncertainty). Conversely, other groups
509 consider that the reproducibility of the standard is a reflection of the external
510 reproducibility of all analyses and that this uncertainty should be incorporated into the
511 uncertainty of each individual analyses of an unknown zircon (Ireland and Williams,
512 2003; Stern and Amelin, 2003). This results in a reduction in the MSWD and has
513 implications for the identification of outliers (Ireland and Williams, 2003).
514 Information regarding the approach taken to the standardisation uncertainty is often
515 recorded in the footnotes to the data table or in the data repository but can be crucial
516 when trying to precisely sequence rocks or calculate durations of events.

517 Typical internal (2σ) uncertainties for ID-TIMS $^{207}\text{Pb}/^{206}\text{Pb}$ and $^{206}\text{Pb}/^{238}\text{U}$ dates are
518 ca. 0.5-0.2% and ca. 0.1-0.05 % respectively, and for microbeam techniques internal
519 (2σ) uncertainties on $^{207}\text{Pb}/^{206}\text{Pb}$ and $^{206}\text{Pb}/^{238}\text{U}$ dates are ca. 3-5% and ca. 1-2%
520 respectively.

521 *5.2 Systematic/external uncertainties*

522 Systematic uncertainties are those related to the uncertainty in absolute value of
523 various constant parameters used in the calculation of either an isotopic ratio or in the
524 calculation of the date itself.

525 *5.2.1 Decay constants*

526 One source of systematic uncertainty that affects all radio-isotopic dates are those
527 related to the uncertainty in the decay constants (Table 1). Three approaches have
528 been taken to determine the decay constants (the probability that a given atom will
529 decay per unit of time) of the long-lived radionuclide; (1) direct counting; (2)
530 ingrowth and (3) geological comparison. Direct counting involves the detection of
531 alpha, beta or gamma activity relative to the total number of radioactive atoms.
532 Ingrowth relies upon the quantification of a decay product that is accumulated from a
533 quantity of high-purity parent nuclide over a well-defined period of time. Geologic
534 comparison involves the analyses of cogenetic materials with multiple chronometers,
535 knowing that each chronometer should yield an equivalent date. This approach has
536 the potential for relative intercalibration of the decay constants but accurate
537 intercalibration requires that at least one decay constant is accurate and known with
538 some precision. This is usually assumed to be the ^{238}U and ^{235}U due to the precision
539 with which the decay constants have been determined (Jaffey et al., 1971) and the
540 internal check provided by closed system zircon analyses (Mattinson, 2000; Schoene
541 et al., 2006).

542 The counting experiments of Jaffey et al (1971) determined the ^{238}U and ^{235}U decay
543 constants with uncertainties of 0.11% and 0.14% respectively. These values have
544 been adopted for use in geochronology (Steiger and Jager, 1977). The ^{187}Re and ^{176}Lu
545 decay constants have been determined by both direct counting experiment and
546 through geologic comparison with the U-Pb system and uncertainties are estimated at
547 ca. 0.4 to 0.5% (Scherer et al., 2001; Selby et al., 2007).

548 The incorporation of decay constant uncertainties are becoming increasingly
549 important as both the internal precision of dates is reduced and multiple
550 geochronometers are being used to investigate the same time intervals. The decay
551 constant uncertainties for isochron dates are typically <20% of the total uncertainty
552 budget, in contrast the uncertainties in the U decay constants are often >50% of the

553 total uncertainty budget of U/Pb ID-TIMS dates (Fig. 2). The situation for the ID-
554 TIMS U/Pb community is that they are now often generating $^{206}\text{Pb}/^{238}\text{U}$ and
555 $^{207}\text{Pb}/^{206}\text{Pb}$ dates that do not overlap within analytical precision and the U decay
556 constant uncertainties have to be considered (Begemann et al., 2001; Ludwig, 2000).
557 As the ‘user’ often uses these date interchangeably we are now seeing $^{206}\text{Pb}/^{238}\text{U}$ and
558 $^{207}\text{Pb}/^{206}\text{Pb}$ age uncertainties as $\pm X/Y/Z$ and $\pm X/Z$ respectively, where X is the
559 analytical/internal uncertainty, Y is the analytical uncertainty plus the systematic
560 tracer calibration uncertainty and Z is the total uncertainty including X, Y and the
561 decay constant uncertainties. This permits use of the data with the level of
562 uncertainty that is appropriate to the problem being addressed.

563 *5.2.2 Age of primary standards for microbeam U/Pb dating*

564 As discussed above, U-Pb microbeam techniques rely upon measurement of the U/Pb
565 ratio relative to standard minerals of known age. The U/Pb dates of these minerals are
566 determined via ID-TIMS analyses with typical total uncertainties of 0.1 to 0.3%
567 which should be propagated into the total uncertainty of the final U/Pb microbeam
568 date. Since the systematic uncertainty related to the age of the primary standard is
569 about an order of magnitude less than the random errors related to the dating of the
570 unknown mineral and often not considered.

571 Intra- and inter-crystal homogeneity is a fundamental requirement of a zircon standard
572 for microbeam U/Pb geochronology as the U/Pb ratio of the standard is considered
573 invariant. Isotopic homogeneity is assessed by multiple ID-TIMS analyses on single
574 crystals and/or crystal fragments (Black et al., 2003; Schmitz et al., 2003) and assess
575 variability on a microgram scale, however microbeam techniques require standards
576 that are homogeneous on the sub-micron scale. At present zircons standards are either
577 chips of megacrysts (e.g., SL13 and 91500) or multi-crystal mineral separates from
578 plutonic rocks (e.g., Temora). In general the zircon standards are relatively
579 homogenous (at the level that can be detected by either microgram ID-TIMS analyses
580 or nanogram SIMS analyses) however there has been issues with at least one of the
581 megacryst standards (SL13) which is heterogeneous at the micron-scale (Ireland and
582 Williams, 2003). The fact that all zircon standards are natural means they are not
583 ideal as they are likely to be affected by zonation and/or Pb-loss and/or other (matrix
584 related) differences which may occur below the level of quantification.

585 5.2.3 Calibrating tracers for isotope-dilution

586 For isotopic analyses that use the addition of isotopic tracers (isotope dilution), the
587 accuracy of the tracer calibration (isotopic composition and concentrations) has a
588 major control on the accuracy of the derived dates for a mineral or rock. Calibration
589 of tracers is performed through admixing the tracer with another solution of known
590 isotopic composition and, importantly, known purity. High-purity metals or salts (see
591 (Selby et al., 2007), for details of a Re-Os tracer; Condon et al., in prep, for details of
592 a U/Pb tracer calibration) are used as the basis the gravimetric reference solutions
593 against which the concentration of the tracer isotope can be determined, therefore the
594 purity of the metal or salt, and the accuracy of the weighing prior to dissolution,
595 controls the precision and accuracy of the calibration. This total uncertainty is
596 typically estimated at ca. 0.1%. For multi-element tracers the elemental (i.e., U/Pb)
597 ratio is fixed therefore the uncertainty in the tracer calibration is systematic and can be
598 ignored for the practical purposes of age determinations generated using the same
599 tracer. This is particularly useful when attempting to determine the relative time
600 difference between samples such as determining sediment accumulation rates
601 (Bowring et al., 2007), or assessing synchronicity of events (Condon et al., 2005). At
602 present it is typical that each isotope laboratory has their own tracer therefore the
603 tracer uncertainty has to be considered when comparing dates with other labs and
604 other techniques. Recently the U/Pb ID-TIMS community has made an effort to
605 eliminate this inter-laboratory uncertainty through the development and calibration of
606 a large amount of ^{205}Pb - ^{233}U - ^{235}U tracer for community use under the auspices of the
607 EARTHTIME Initiative (Condon et al., in prep).

608 5.3 Calculating an age from multiple dates

609 A significant proportion of age constraints for Neoproterozoic strata are U-Pb dates
610 on zircons from extrusive (volcanic) or intrusive igneous rocks. The final reported
611 date and associated uncertainty are commonly *weighted mean* dates derived from a
612 number (n) of individual dates on different zircons (or zircon sub-domains), and
613 commonly calculated using the algorithms in the Isoplot software (Ludwig, 1991).
614 This is the case for data acquired using both ID-TIMS and microbeam techniques.
615 The weighted mean is favoured as it weights each individual analyses (such as a
616 single SIMS spot or single grain ID-TIMS analyses) according to its precision so
617 analyses with a low uncertainty (high weight) contribute more to the weighted mean

618 than do elements with a high uncertainty (low weight). Importantly, the use of a
619 weighted mean algorithm (or other averaging) is underpinned by the expectation of a
620 single population with normally distributed errors. If the errors on the individual
621 analyses are approximately equal (as is typical for microbeam U/Pb data) then the
622 weighted mean uncertainty is proportional to $1/\sqrt{n}$, therefore high- n datasets can be
623 used to reduce the overall age uncertainty for data collected on a single population
624 with normally distributed errors. If the uncertainties on the individual analyses are
625 variable (as is common in ID-TIMS U/Pb data with a range of Pb^*/Pb_c ratios) then the
626 weighted mean uncertainty is controlled by the few most precise analyses, however
627 the high- n dataset is critical for assessing the spread of dates from a given sample.

628 A common measure of the “coherence” of a data set is a statistical parameter called
629 the MSWD (mean square of the weighted deviates; (York, 1966, 1967). A value of
630 approximately 1 indicates that the scatter in the data can be explained by analytical
631 uncertainties alone, values much less than 1 indicates that analytical uncertainties
632 have been overestimated, and values greater than 1 can indicate either that the
633 uncertainties have been underestimated or that another source of scatter, often called
634 “geological” scatter is present. Although not often explicitly stated, an MSWD of 1
635 does not necessarily mean there is a single age population. Rather, it indicates that if
636 real age variation is present, it cannot be resolved within the precision of the
637 individual analyses.

638 ***5.4 Uncertainties as a result of geologic complexity***

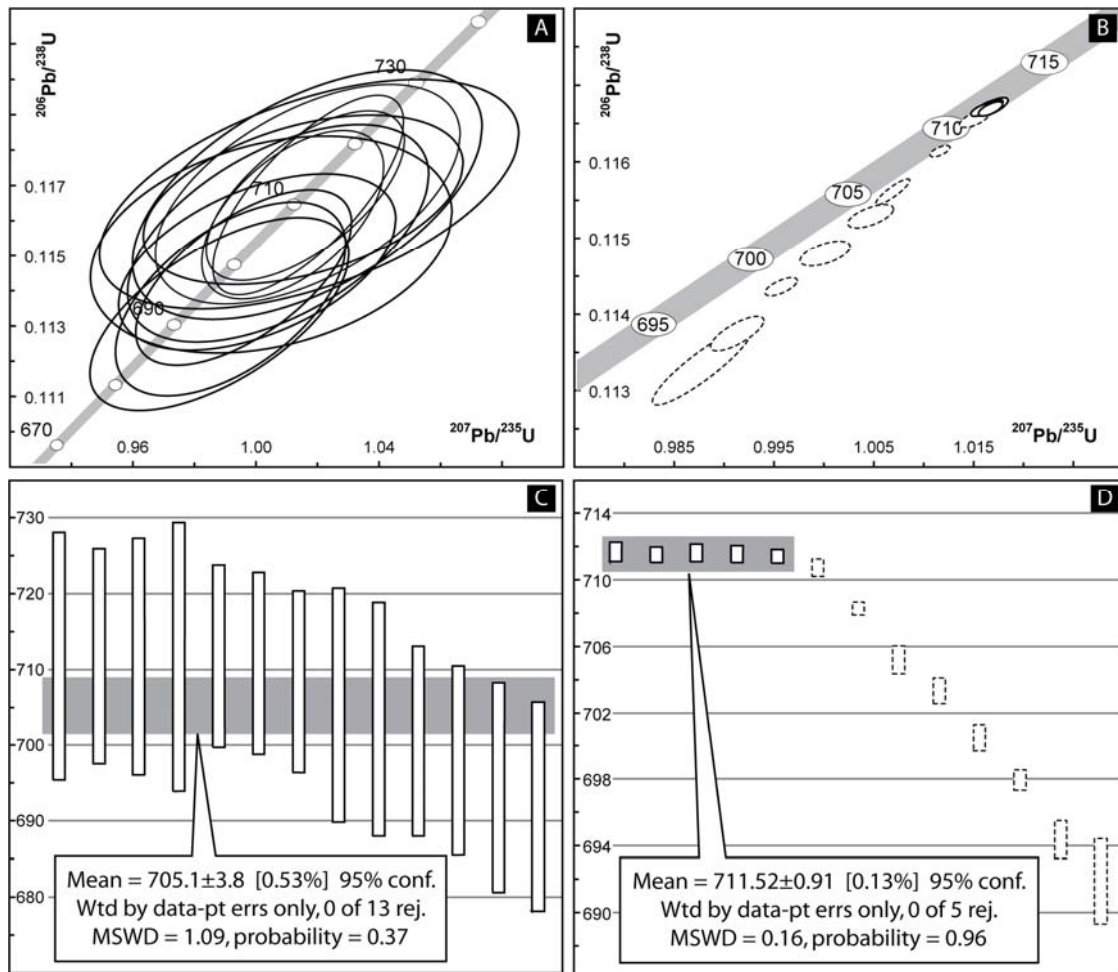
639 Uncertainty as a result of geologic complexity is the most difficult to quantify. The
640 most common cause of excess scatter is open system behaviour resulted from either
641 inheritance of older zircon or Pb loss. For U-Pb zircon analyses reduced errors on
642 single analyses often exposes fine-scale variability that may reflect protracted growth
643 of zircon crystals in a magma chamber or the effects of very subtle open system
644 behaviour thus that high-precision analyses do not always transform into reduced
645 uncertainties in calculated weighted mean dates.

646 ***5.4.1 Complex U-Pb zircon systematics***

647 In the past decade errors associated with ID-TIMS analyses have dropped by almost
648 an order of magnitude and while this is good it also exposes complexity at the $<0.1\%$
649 level sometimes resulting in scatter and higher values of MSWD. It is now common

650 for the geochronologist to be faced with a population of zircon analyses that do not
651 form a coherent cluster (MSWD = 1) and the crucial question is how to interpret the
652 data to arrive at a depositional age. The advent of CA-TIMS pre-treatment for the
653 elimination of Pb-loss has been extremely important as it gives one confidence that in
654 many cases Pb-loss need not be considered as a cause of excess scatter. Furthermore,
655 for Neoproterozoic rocks, the concordia curve has a shallow enough slope, and the
656 $^{207}\text{Pb}/^{235}\text{U}$ dates measured precisely enough to be able to evaluate discordance at the
657 per mil level, however this is not the case for microbeam U/Pb dates.

658 As outlined above, microbeam U/Pb dates on volcanic rocks rely upon the averaging
659 of a relatively high- n dataset (10-20) of relatively imprecise (ca. 2 to 4%) U/Pb
660 determinations to get a weighted mean date with precision ca. 1%. Underpinning
661 these lower uncertainties is the assumption of a single population with normally
662 distributed errors. However, it is the low precision of each analysis combined with
663 variability of the standard analyses that bracket unknowns that often precludes the
664 detection of subtle amounts of Pb loss or inheritance. Stated another way, if the
665 amount of Pb-loss or inheritance is less than the precision of a single spot analyses
666 then it cannot be detected via normal statistical proxies (such as the MSWD) therefore
667 the assumption of a normal distribution maybe be invalid (see Fig. 4). If Pb-loss is
668 the main source of open-system behaviour, this will have the effect of lowering the
669 $^{206}\text{Pb}/^{238}\text{U}$ date on some analyses as well as the weighted mean $^{206}\text{Pb}/^{238}\text{U}$ date (Fig.
670 4). The inability to detect small amounts of Pb loss in small volumes of zircon
671 analyzed by microbeam techniques represents a significant limitation for their
672 application to high precision geochronology (Bowring et al., 2006).



673

674 **Figure 4.** U-Pb concordia and weighted mean $^{206}\text{Pb}/^{238}\text{U}$ plots for a somewhat synthetic dataset.
 675 Plotted are U/Pb ratios (A and B) and $^{206}\text{Pb}/^{238}\text{U}$ dates (C and D). A and C are analyses with typical 2σ
 676 ‘microbeam’ (1.5 to 2.5% for $^{206}\text{Pb}/^{238}\text{U}$ and 2.4 to 5.5% for the $^{207}\text{Pb}/^{235}\text{U}$ ratio) the uncertainties
 677 whereas B and D are the exact same analyses with typical ID-TIMS uncertainties (0.06 to 0.16% for
 678 $^{206}\text{Pb}/^{238}\text{U}$ and 0.09 to 0.22% for the $^{207}\text{Pb}/^{235}\text{U}$ ratio). Weighted mean ID-TIMS $^{206}\text{Pb}/^{238}\text{U}$ date include
 679 a 0.1% uncertainty in the U/Pb of the tracer. All error ellipses and error boxes are plotted at 2σ level.

680

681 In-situ techniques are without question essential tools for characterizing complex
 682 zircons from volcanic and metamorphic rocks and for sifting through detrital
 683 populations to characterise source areas and in some cases provide robust estimates of
 684 the minimum age of a sequence. Ideally, microbeam techniques would be used to
 685 rapidly characterise a population of zircons by analyzing a small volume of many
 686 zircons, which could then be followed by conventional high-precision geochronology
 687 of selected grains.

688 *5.4.1 Non-simple Isochrons*

689 As outlined above, a limitation of the ‘isochron geochronometers’ is the lack of an
690 independent check for ‘open-system’ behaviour, unlike the dual decay scheme of the
691 U-Pb system. Most studies employ a combination of bracketing age constraints
692 and/or a statistical measure of coherence (MSWD or uncertainty) to assess whether
693 the system has been perturbed, however precision and amount of scatter cannot be
694 used as a proxy for closed system behaviour. For example, organic rich sediments
695 from the Aralka Formation, Australia, have been analysed for Re-Os geochronology
696 using both the aqua regia and CrO₃-H₂SO₄ dissolution methods. Schaffer and
697 Burgess (Schaefer and Burgess, 2003) used the aqua regia dissolution method and
698 obtained a 3 point isochron (samples integrated over 1.6 m stratigraphic thickness) of
699 592 ± 14 Ma (MSWD $\ll 1$). An expanded dataset collected over 10m stratigraphic
700 thickness yielded a 9 point regression and an age of 623 ± 18 Ma (MSWD = 5.2).
701 Subsequent Re-Os analyses (on samples from a 2 m interval within the 10m interval
702 sampled by Schaffer and Burgess., 2003) using the CrO₃-H₂SO₄ dissolution method
703 yielded a 10 point isochron with an age of 657.2 ± 5.4 Ma (2σ internal uncertainties,
704 MSWD = 1.2) (Kendall et al., 2006). This difference is attributed to either a sampling
705 and/or analytical artefact related to sample digestion (Kendall et al., 2006).

706 It is clear from the Alralka case study that care must be taken when using coherence
707 of a dataset as means to assess the accuracy, especially with isochrones based upon
708 low-*n* datasets. The bottom line is that a suite of samples with the same initial ratio
709 and a range of parent daughter ratios that evolve in a closed system yield an isochron
710 but if a suite of samples define a statistically significant linear array one cannot
711 necessarily infer closed system behaviour as simple mixing of two reservoirs can
712 yield linear arrays.

713

714 **6. Conclusions**

715 (a) *There are a number of radio-isotopic dating techniques that can be employed to*
716 *constrain the age of a sedimentary succession.* These include U-Pb dating of minerals
717 from volcanic rocks which date the eruption, to Re-Os or U-Pb ‘isochron’ dating of
718 organic-rich sediments or carbonates. The suitability of a given technique is governed
719 by the geological material. Most Neoproterozoic age constraints are based upon U-Pb

720 zircon dates from extrusive igneous rocks, this dataset is augmented by a growing
721 number of Re-Os, Pb-Pb and Lu-Hf isochron dates.

722 Each of the radio-isotopic systems have different strengths and weaknesses, mainly
723 relating to the specific type of material needed for analyses and its presence in the
724 stratigraphic section of interest. U-Pb (zircon) dating is considered the premier
725 geochronometer however it is of limited use in successions devoid of zircon bearing
726 volcanics. Realising the goal of a robust and highly-resolved temporal framework for
727 the Neoproterozoic will require exploitation of all these different methodologies.

728 *(b) All dates are underpinned by a series of assumptions and include a component of*
729 *interpretation.* Radio-isotopic dates such as U-Pb (zircon) dates from volcanic rocks
730 and isochron dates from sediments are based upon datasets that comprise a number of
731 separate analyses. In the case of U-Pb (zircon) dates from volcanic rocks, the final
732 product is usually a weighted mean $^{206}\text{Pb}/^{238}\text{U}$ date in which a number (up to ca. 15)
733 of single $^{206}\text{Pb}/^{238}\text{U}$ dates (either single grain or single spot analyses) are weighted
734 (based upon their associated uncertainty) and a mean calculated. Underpinning this
735 mean date, and its lower uncertainty (about 2 to 4 times lower than the uncertainty on
736 a single analyses), is the assumption of a single population with normally distributed
737 errors. Isochron dates are similarly based upon the linear regression through a
738 number of data points that are assumed to be cogenetic, have a common initial
739 daughter isotopic composition, and that the materials analysed have acted as a 'closed
740 system' since their formation.

741 *(c) The uncertainty of the date is no less significant than the date itself.* The total
742 uncertainty of a radio-isotopic date comprises random, or internal, and systematic
743 components. The random/internal uncertainties are related to the measurement of the
744 isotopic ratios and the corrections applied. Systematic uncertainties are those related
745 to the uncertainty in absolute value of various constant parameters used in the
746 calculation of either an isotopic ratio or in the calculation of the date itself. Analytical
747 uncertainties should reflect the ability to reproduce a given isotopic ratio and
748 represent the minimum uncertainty that should be considered. For microbeam U/Pb
749 dates the standard calibration is best considered as a non-systematic uncertainty and
750 should be incorporated into each individual U/Pb date uncertainty (Ireland and
751 Williams, 2003). If comparing dates generated using different techniques or using
752 different calibration materials (such as mineral standards for microbeam dates of

753 isotopic tracer for ID-TIMS) then the systematic uncertainties related to these
754 calibrations must be considered. An additional systematic uncertainty is that related
755 to the decay constants used in the age calculation. These uncertainties have been
756 determined experimentally or assessed via geological comparison with another decay
757 scheme. There is considerable variation in the published literature regarding the
758 treatment of the constituent parts of the total uncertainty budget. In some cases, such
759 as using ID-TIMS $^{206}\text{Pb}/^{238}\text{U}$ dates generated using a single isotopic tracer solution,
760 certain components can be ignored (in this case tracer calibration uncertainty and ^{238}U
761 decay constant uncertainty). This can be useful when attempting to determine
762 sediment accumulation rates or assess the synchronicity of events.

763 Although there is a desire for a date with the lowest possible uncertainty, the high-
764 precision is most beneficial when considered in the context of the single analyses. It
765 is the precision of the single analyses that controls our ability to assess the occurrence
766 of ‘open-system’ behaviour and thus the accuracy of the final date. Although the
767 coherence of a dataset is often used as a proxy for closed-system behaviour, the
768 coherence is limited by the precision of the individual analyses.

769

770 **Acknowledgements**

771 All U-Pb plots and calculations were preformed using Isoplot
772 (http://www.bgc.org/isoplot_etc/software.html).

773 **6. References Cited.**

- 774 Babinski, M., Van Schmus, W.R., and Chemale, F., 1999, Pb-Pb dating and Pb
775 isotope geochemistry of Neoproterozoic carbonate rocks from the Sao
776 Francisco basin, Brazil: implications for the mobility of Pb isotopes during
777 tectonism and metamorphism: *Chemical Geology*, v. 160, p. 175-199.
- 778 Babinski, M., Vieira, L.C., and Trindade, R.I.F., 2007, Direct dating of the Sete
779 Lagoas cap carbonate (Bambui Group, Brazil) and implications for the
780 Neoproterozoic glacial events: *Terra Nova*, v. 19, p. 401-406.
- 781 Barfod, G.H., Albarede, F., Knoll, A.H., Xiao, S.H., Telouk, P., Frei, R., and Baker,
782 J., 2002, New Lu-Hf and Pb-Pb age constraints on the earliest animal fossils:
783 *Earth and Planetary Science Letters*, v. 201, p. 203-212.
- 784 Begemann, F., Ludwig, K.R., Lugmair, G.W., Min, K., Nyquist, L.E., Patchett, P.J.,
785 Renne, P.R., Shih, C.Y., Villa, I.M., and Walker, R.J., 2001, Call for an
786 improved set of decay constants for geochronological use: *Geochimica Et*
787 *Cosmochimica Acta*, v. 65, p. 111-121.
- 788 Bingen, B., Griffin, W.L., Torsvik, T.H., and Saeed, A., 2005, Timing of Late
789 Neoproterozoic glaciation on Baltica constrained by detrital zircon
790 geochronology in the Hedmark Group, south-east Norway: *Terra Nova*, v. 17,
791 p. 250-258.
- 792 Black, L.P., Kamo, S.L., Allen, C.M., Aleinikoff, J.N., Davis, D.W., Korsch, R.J., and
793 Foudoulis, C., 2003, TEMORA 1: a new zircon standard for Phanerozoic U-
794 Pb geochronology: *Chemical Geology*, v. 200, p. 155-170.
- 795 Bowring, S.A., Grotzinger, J.P., Condon, D.J., Ramezani, J., Newall, M., and Allen,
796 P.A., 2007, Geochronologic constraints of the chronostratigraphic framework
797 of the Neoproterozoic Huqf Supergroup, Sultanate of Oman: *American*
798 *Journal of Science*, v. 307, p. 1097-1145.
- 799 Bowring, S.A., Schoene, B., Crowley, J.L., Ramezani, J., and Condon, D.J., 2006,
800 High-precision U-Pb zircon geochronology and the stratigraphic record:
801 progress and promise: *The Paleontological Society Papers*, v. 12, p. 25-46.
- 802 Condon, D., Zhu, M.Y., Bowring, S., Wang, W., Yang, A.H., and Jin, Y.G., 2005, U-
803 Pb ages from the neoproterozoic Doushantuo Formation, China: *Science*, v.
804 308, p. 95-98.

805 Creaser, R.A., Sannigrahi, P., Chacko, T., and Selby, D., 2002, Further evaluation of
806 the Re-Os geochronometer in organic-rich sedimentary rocks: A test of
807 hydrocarbon maturation effects in the Exshaw Formation, Western Canada
808 Sedimentary Basin: *Geochimica Et Cosmochimica Acta*, v. 66, p. 3441-3452.

809 Evans, J.A., Zalasiewicz, J.A., Fletcher, I., Rasmussen, B., and Pearce, N.J.G., 2002,
810 Dating diagenetic monazite in mudrocks: constraining the oil window?:
811 *Journal of the Geological Society*, v. 159, p. 619-622.

812 Halverson, G.P., Hoffman, P.F., Schrag, D.P., Maloof, A.C., and Rice, A.H.N., 2005,
813 Toward a Neoproterozoic composite carbon-isotope record: *Geological*
814 *Society Of America Bulletin*, v. 117, p. 1181-1207.

815 Ireland, T.R., Flottmann, T., Fanning, C.M., Gibson, G.M., and Preiss, W.V., 1998,
816 Development of the early Paleozoic Pacific margin of Gondwana from
817 detrital-zircon ages across the Delamerian orogen: *Geology*, v. 26, p. 243-246.

818 Ireland, T.R., and Williams, I.S., 2003, Considerations in Zircon Geochronology by
819 SIMS: *Reviews in Mineralogy and Geochemistry*, v. 53, p. 215-241.

820 Jaffey, A.H., Flynn, K.F., Glendenin, L.E., Bentley, W.C., and Essling, A.M., 1971,
821 Precision measurement of half-lives and specific of ^{235}U and ^{238}U : *Physics*
822 *Reviews*, v. C4, p. 1889-1906.

823 Kendall, B., Creaser, R.A., and Selby, D., 2006, Re-Os geochronology of postglacial
824 black shales in Australia: Constraints on the timing of "Sturtian" glaciation:
825 *Geology*, v. 34, p. 729-732.

826 Kendall, B.S., Creaser, R.A., Ross, G.M., and Selby, D., 2004, Constraints on the
827 timing of Marinoan "Snowball Earth" glaciation by Re-187-Os-187 dating of a
828 Neoproterozoic, post-glacial black shale in Western Canada: *Earth And*
829 *Planetary Science Letters*, v. 222, p. 729-740.

830 Kosler, J., and Sylvester, P.J., 2003, Present trends and the future of zircon in
831 geochronology: *Laser ablation ICPMS: Zircon*, v. 53, p. 243-275.

832 Krogh, T.E., 1982a, Improved accuracy of U-Pb zircon ages by the creation of more
833 concordant zircon systems using an air abrasion technique: *Geochimica Et*
834 *Cosmochimica Acta*, v. 46, p. 637-649.

835 —, 1982b, Improved Accuracy of U-Pb Zircon Dating by Selection of More
836 Concordant Fractions Using a High-Gradient Magnetic Separation Technique:
837 *Geochimica Et Cosmochimica Acta*, v. 46, p. 631-635.

838 Ludwig, K.R., 1980, Calculation of Uncertainties of U-Pb Isotope Data: Earth and
839 Planetary Science Letters, v. 46, p. 212-220.

840 —, 1991, Isoplot - a plotting and regression program for radiogenic isotope data:
841 USGS Open File Report, p. 91-445.

842 —, 1998, On the treatment of concordant uranium-lead ages: *Geochimica Et*
843 *Cosmochimica Acta*, v. 62, p. 665-676.

844 —, 2000, Decay constant errors in U-Pb concordia-intercept ages: *Chemical Geology*,
845 v. 166, p. 315-318.

846 —, 2003, Mathematical-Statistical Treatment of Data and Errors for $^{230}\text{Th}/\text{U}$
847 Geochronology: *Reviews in Mineralogy and Geochemistry*, v. 52, p. 631-656.

848 Mattinson, J.M., 2000, Revising the "gold standard" - the Uranium decay constants of
849 Jaffey et al., 1971.: EOS, AGU Fall meeting Supplement Abstract V61A-02.

850 —, 2005, Zircon U-Pb chemical abrasion ("CA-TIMS") method: Combined annealing
851 and multi-step partial dissolution analysis for improved precision and accuracy
852 of zircon ages: *Chemical Geology*, v. 220, p. 47-66.

853 Peterson, K.J., McPeck, M.A., and Evans, D.A.D., 2005, Tempo and mode of early
854 animal evolution: inferences from rocks, Hox, and molecular clocks:
855 *Paleobiology*, v. 31, p. 36-55.

856 Rasmussen, B., 2005, Radiometric dating of sedimentary rocks: the application of
857 diagenetic xenotime geochronology: *Earth-Science Reviews*, v. 68, p. 197.

858 Schaefer, B.F., and Burgess, J.M., 2003, Re-Os isotopic age constraints on deposition
859 in the Neoproterozoic Amadeus Basin: implications for the 'Snowball Earth':
860 *Journal of the Geological Society*, v. 160, p. 825-828.

861 Scherer, E., Munker, C., and Mezger, K., 2001, Calibration of the lutetium-hafnium
862 clock: *Science*, v. 293, p. 683-687.

863 Schmitz, M.D., Bowring, S.A., and Ireland, T.R., 2003, Evaluation of Duluth
864 Complex anorthositic series (AS3) zircon as a U-Pb geochronological
865 standard: New high-precision isotope dilution thermal ionization mass
866 spectrometry results: *Geochimica Et Cosmochimica Acta*, v. 67, p. 3665-3672.

867 Schmitz, M.D., and Schoene, B., 2007, Derivation of isotope ratios, errors, and error
868 correlations for U-Pb geochronology using $\text{Pb-}^{205}\text{-U-}^{235}\text{-(U-}^{233}\text{)}$ -spiked
869 isotope dilution thermal ionization mass spectrometric data: *Geochemistry*
870 *Geophysics Geosystems*, v. 8, p. -.

871 Schoene, B., Crowley, J.L., Condon, D.J., Schmitz, M.D., and Bowring, S.A., 2006,
872 Reassessing the uranium decay constants for geochronology using ID-TIMS
873 U-Pb data: *Geochimica Et Cosmochimica Acta*, v. 70, p. 426-445.

874 Selby, D., Creaser, R.A., Stein, H.J., Markey, R.J., and Hannah, J.L., 2007,
875 Assessment of the Re-187 decay constant by cross calibration of Re-Os
876 molybdenite and U-Pb zircon chronometers in magmatic ore systems:
877 *Geochimica Et Cosmochimica Acta*, v. 71, p. 1999-2013.

878 Steiger, R.H., and Jager, E., 1977, Subcommission on Geochronology - Convention
879 on Use of Decay Constants in Geochronology and Cosmochronology: *Earth
880 and Planetary Science Letters*, v. 36, p. 359-362.

881 Stern, R.A., and Amelin, Y., 2003, Assessment of errors in SIMS zircon U-Pb
882 geochronology using a natural zircon standard and NIST SRM 610 glass:
883 *Chemical Geology*, v. 197, p. 111-142.

884 York, D., 1966, Least Squares fitting of a straight line: *Canadian Journal of Physics*,
885 v. 44, p. 1079-1086.

886 —, 1967, The best isochron: *Earth and Planetary Science Letters*, v. 2, p. 479-482.

887 Zhou, C., Tucker, R., Xiao, S., Peng, Z., Yuan, X., and Chen, Z., 2004, New
888 constraints on the ages of Neoproterozoic glaciations in south China: *Geology*,
889 v. 32, p. 437-440.

890

891